# LEGIBILITY NOTICE

A major purpose of the Technical Information Center is to provide the broadest dissemination possible of information contained in DOE's Research and Development Reports to business, industry, the academic community, and federal, state and local governments.

Although a small portion of this report is not reproducible, it is being made available to expedite the availability of information on the research discussed herein.

Los Alamos National Laboratory is operated by the University of California for the United States Department of Energy under contract W-7405 ENG 36

LA-UR--89-1457

DE89 011166

TITLE: FISSION BARRIERS AND HALF-LIVES

AUTHOR(S): P. Moller, J. R. Nix, and W. J. Swiatecki

SUBMITTED TO: For presentation at the American Nuclear Society and National Institute of Standards and Technology Conference on Fifty Years with Nuclear Fission, Gaithersburg, Maryland, April 25-28, 1989

## DISCLAIMER





Los Alamos Los Alamos National Laboratory
Los Alamos, New Mexico 87545

# FISSION BARRIERS AND HALF-LIVES

P. Möller, J. R. Nix
Theoretical Division, MS B279
Los Alamos National Laboratory
Los Alamos, NM 87545
(505) 667-6228

W. J. Swiatecki
Nuclear Science Division, 70A-3307
Lawrence Berkeley Laboratory
Berkeley, CA 94720
(415) 486-5536

ABSTRACT

We briefly review the development of theoretical models for the calculation of fission barriers and half-lives. We focus on how results of actual calculations in a unified macroscopic-microscopic approach provide an interpretation of the mechanisms behind some of the large number of phenomena observed in fission. As instructive examples we choose studies of the rapidly varying fission properties of elements at the end of the periodic system.

## INTRODUCTION

The history of fission is often that of an unexpected experimental discovery followed by theoretical interpretations. In 1934 Fermi bombarded uranium with neutrons and and erroneously concluded that transuranium elements had been produced. Noddack[1] correctly suggested that fission had been observed, but the credit for discovering fission goes to Hahn and Straßmann, who in 1938 repeated Fermi's experiments and clearly identified barium in the reaction products. Soon afterwards Meitner and Frisch[2] interpreted this reaction as a breakup of the uranium nucleus into two smaller fragments, resulting from the Coulomb repulsion overcoming the stabilizing influence of the surface tension. This analogy with a charged liquid drop was also discussed by others and developed into a more complete theory by Bohr and Wheeler.[3]

The first 25 years of fission theory, which are very much the history of the liquid-drop model, are being reviewed in other contributions at this conference. Although the liquid-drop model accounts for many features of the fission process it leaves others unexplained, for instance the mass asymmetry and the variation of half-lives in actinide fission. The last 25 years of fission theory have seen how the liquid-drop picture has been modified to account for many of these phenomena. Also some of these developments are being reviewed at this conference.

The big leap forward in our understanding of the fission process occurred in the mid 1960's, when the effects of microscopic nuclear structure on the fission process came into focus. However, preliminary steps in this direction were taken earlier. Just as irregularities in nuclear masses could be understood in terms of the extra stability associated with magic numbers, it was realized by Swiatecki[4] in 1955 that it was possible to account for the variation in actinide fission half-lives by adding a shell correction to the fission-barrier ground-state minimum given by the liquid-drop model. This shell correction was calculated as the difference between the mass calculated in the liquid-drop model and the experimental mass. At the same time, the increased stability towards fission of odd nuclei was explained[5,6] in terms of a specialization energy due to the conservation of spin of the odd particle during the barrier penetration process. These two developments showed that shell effects could be important both at the nuclear ground state and at larger deformations corresponding to saddle-point shapes. Later, Johansson[7] tried to estimate shell effects from calculated single-particle levels in a deformed potential well.

However, it was work by Strutinsky,[8,9] stimulated by the earlier discovery of fission-isomeric states, that led to a well-defined method for calculating the shell correction. In the years 1966–1973 this method resulted in an enormous theoretical activity in the study of fission properties. Based on calculated potential-energy surfaces, fission isomeric states[8] and the mechanism of mass-asymmetric fission[10] were explained and fission half-lives were determined.[11,12] Speculation on the existence of a superheavy island near $Z = 114$ was more quantitatively investigated in several extensive calculations.[13–15]

## MODELS

To determine fission-barrier heights, the potential energy of a nucleus is calculated for a prescribed set of shapes. In the simplest case the shapes may be characterized in terms of *one* shape coordinate. The potential energy displayed in terms of this coordinate is the *fission barrier*. Fission half-lives are given by the penetrability through this one-dimensional barrier

In the more general case, the energy is calculated in

terms of several shape coordinates, for example elongation, neck radius and mass asymmetry. Precisely how these variables should be defined is a difficult and important problem. In the multi-dimensional case a fission barrier is not a well-defined concept. Fission half-lives should, in principle, be calculated by considering the penetration of the multi-dimensional potential-energy surface in some model. This general case is extremely complicated and has never been treated exactly.

The usual approach is to display two-dimensional subspaces of the multi-dimensional potential-energy calculations as *potential-energy surfaces* in terms of two shape coordinates. One coordinate is usually chosen to be related to elongation, the other to mass asymmetry or to neck size. In the multi-dimensional case a fission barrier is usually defined as the energy along a one-dimensional path through the minima and saddle points in the multi-dimensional space. Since there are an infinite number of paths that pass through the maxima and minima only the extremum points of the barrier are well-defined. Some calculations of fission half-lives consider the penetrability along all possible paths between the ground state and scission. The path with the maximum penetrability corresponds to the path actually taken by the nucleus. In such a treatment the path need not pass through the minima and saddle points of the potential energy.

Two different general classes of models are used to calculate the nuclear potential energy of deformation. The more fundamental models are the self-consistent ones, for instance the Hartree-Fock approximation with an effective two-body interaction. Because of their computational complexity, their full impact has yet to be realized. Most results are obtained by use of the macroscopic-microscopic method. In this approach the energy is given by

$$E_{\rm pot}(\text{shape}) = E_{\rm macr}(\text{shape}) + E_{\rm micr}(\text{shape}) \qquad (1)$$

where the total potential energy $E_{\rm pot}$ is a function of shape and is the sum of a macroscopic term $E_{\rm macr}$ and a microscopic term $E_{\rm micr}$. The macroscopic term gives the binding energy of a nucleus to within about 10 MeV out of a total of 2000 MeV for a heavy nucleus. It describes the smooth trends of the energy as a function of $Z$, $A$ and deformation, whereas the microscopic term accounts for internal structure effects that are, for instance, exhibited as nonuniformities in calculated single-particle level spectra. Thus, the gaps associated with the magic numbers $Z = 82$ and $N = 126$ of spherical $^{208}$Pb are associated with a microscopic energy of about $-12$ MeV. The macroscopic energy is calculated in a model such as the liquid drop model,[16] the droplet model[17,18] or the Yukawa-plus-exponential model[19] and the microscopic term is evaluated from a calculated single particle level spectrum by use of Strutinsky's shell-correction method. This approach has been enormously successful over the past quarter century in describing many aspects of nuclear structure, such as ground-state masses and shapes, fission-barrier heights and fission half-lives, for nuclei throughout the periodic system.

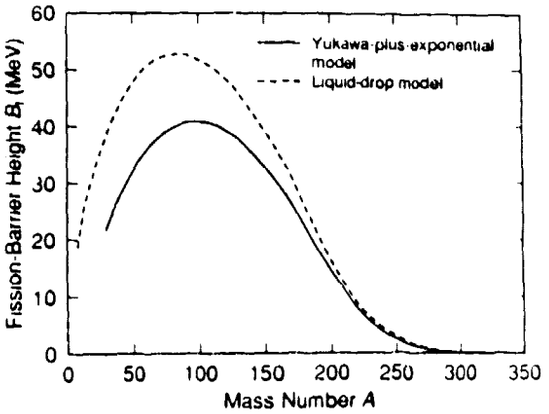


Figure 1: Macroscopic fission-barrier heights in two models. The Yukawa-plus-exponential model agrees much better with experimental data.

There are several models that can be used for each of the two terms in the expression for the total potential energy. The macroscopic term may, for example, be evaluated from a liquid-drop model, a droplet model or a Yukawa-plus-exponential model and the microscopic term from single-particle levels calculated in a Nilsson modified-oscillator one- or two-center potential, a Woods-Saxon potential or a folded-Yukawa single-particle potential. Some properties are well described over a limited region of nuclei by any model combination since the parameters of the models are determined by adjustments to data. However, to obtain a model that can be reliably extrapolated to unknown regions of nuclei and that may predict unexpected features in known regions of nuclei, one should use a unified approach in which a model with a single parameter prescription describes as many nuclear-structure features as possible over the entire periodic system. One such combination is the Yukawa-plus exponential model coupled with the folded-Yukawa single-particle potential. Most of the results we show here are obtained by this combination.

In early 1970's it became clear that the usual surface-energy term in the liquid drop model, namely a term proportional to the surface area of the nucleus, was inadequate for the description of the surface energy of saddle-point shapes with well-developed necks or the surface energy of two colliding heavy ions at a distance within the range of the nuclear force. In particular, the liquid drop model predicted that nuclei in the vicinity of $A = 100$ would have a fission barrier about 55 MeV high, whereas experimental results indicated that the barriers in this

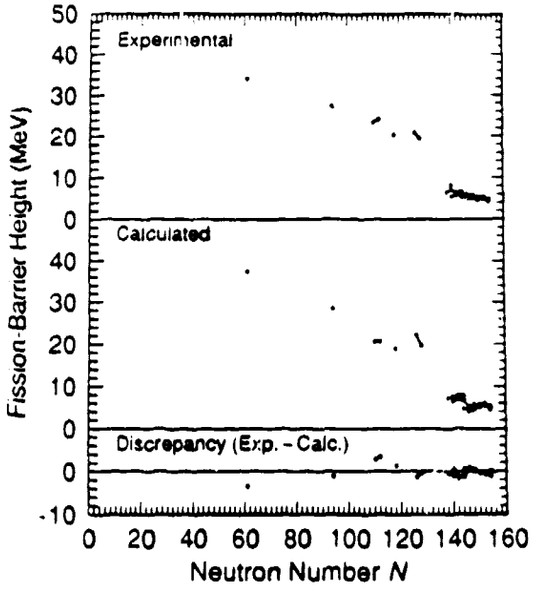


Figure 2: Calculated fission-barrier heights compared to experimental data. For actinide nuclei the second peak in the barrier is the one studied.

region were only about 35 MeV high. This discrepancy could not be removed by any reasonable readjustment of the liquid-drop model parameters.

The proximity-force model[20] was a first step in accounting for the reduction in surface tension due to the finite range of the nuclear force for heavy ions close to the touching configuration. Later, a more general model that can be applied to arbitrary nuclear shapes was developed. In this approach the surface energy is calculated by means of a double volume integral of a Yukawa-plus-exponential function over the nuclear volume.[19]

In fig. 1 we show fission-barrier heights for nuclei on the line of $\beta$-stability calculated in a liquid-drop model and in the Yukawa-plus-exponential model. In the actinide region the two models give very similar results, but in the region $A \approx 100$ the difference is more than 15 MeV. The Yukawa-plus-exponential model agrees well with experiment in this region, whereas it is not possible to bring the liquid-drop model into agreement with data, even with unrealistic choices of the model parameters. This is a reflection of the fact that the saddle-point shapes in the region $A \approx 100$ correspond to shapes with pronounced necks. Models in which the surface energy is simply proportional to the surface area of the deformed nucleus, such as the liquid-drop model, severely overestimate the surface energy for such shapes.

Although the most commonly used single-particle potentials all give similar results in some applications, the folded-Yukawa single-particle potential has a number of distinct advantages. Relative to oscillator-model potentials, its spin-orbit and diffuseness parameters vary slowly and predictably over the periodic system. Relative to the Woods-Saxon model the description of the potential generalizes more naturally to deformed shapes and to separated fragments. Both spherical and deformed ground-state shapes and shapes that occur later in the fission process can be generated with existing shape parameterizations. For instance, the shape of two touching spheres, which is crucial for the study of fission of heavy fermium isotopes, is precisely generated within the shape parameterization.

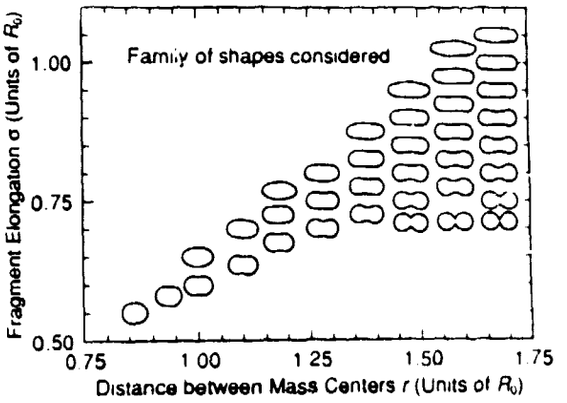


Figure 3: Nuclear shapes corresponding to potential-energy surfaces. The end parts of the shape are kept spherical. The upper boundary corresponds approximately to spheroids and the lower boundary to two overlapping spheres for $r \leq 1.59$ and to scission configurations for $r \geq 1.59$.

## FISSION BARRIERS AND HALF-LIVES

To illustrate the level of understanding of the fission process that is achieved at present in theoretical studies we discuss some results that have been obtained by use of the macroscopic-microscopic method, with the Yukawa-plus-exponential macroscopic model and the folded-Yukawa single-particle model. The focus will be on the very heaviest elements, for which the rapidly changing fission properties present a challenge to the theoretical models. Because of lack of space we have to refer to our more extensive presentations[21,22] for a more complete discussion of our results and the results of other groups.

Fission barriers for actinide nuclei have been quite well reproduced in theoretical calculations already in the early 1970's. The proceedings[23] of the fission conference in Rochester in 1973 give excellent examples of such studies. There are fewer examples of calculations that reproduce fission barriers for elements throughout the periodic system. In fig. 2 we show results of one such calculation taken from a study that adjusted the parameters of the

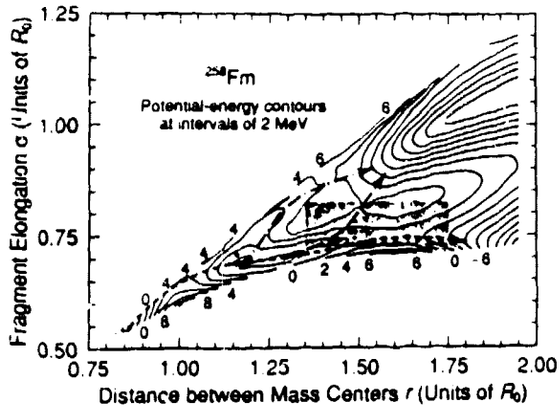


Figure 4: Potential-energy surface corresponding to shapes in fig. 3. The paths correspond, going downwards in the figure, to the old path, the switchback path, and the new path. The stability of the shaded area with respect to mass asymmetry is investigated below.

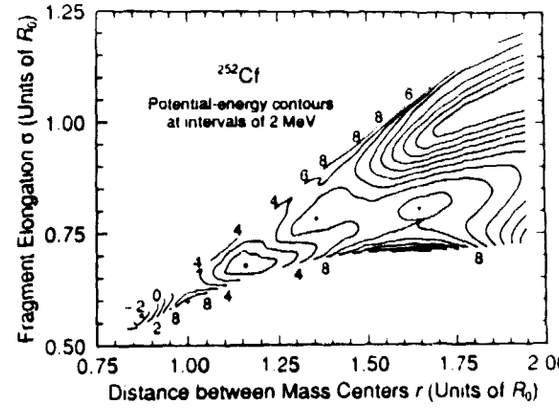


Figure 5: Potential-energy surface for which access to the new valley is blocked by a ridge.

Yukawa-plus-exponential model to ground-state masses and fission barriers throughout the periodic system. The rms deviation between calculated and experimental barrier heights is 1.33 MeV for 28 fission barriers. Also barriers in the region $A \approx 100$ are well reproduced.

Experimental results on the fission properties of actinide nuclei have, until recently, shown that many fission properties vary fairly smoothly from the beginning of the actinide region towards the heaviest known nuclei. However, results obtained over the last 10 to 15 years show that for nuclei close to $^{258}$Fm there are very rapid fluctuations in fission half-lives, kinetic energies and mass asymmetry. The history of these discoveries and details of the experimental data are reviewed by Hoffman and by Hulet in other contributions to this conference. For $^{258}$Fm the mass distribution is sharply symmetric, the spontaneous-fission half-life is short (only 0.38 ms), and the kinetic energy distribution has peaks at 200 and 235 MeV. Hulet *et al.*[24] interpreted the bimodal character of the kinetic-energy distribution to show that for $^{258}$Fm there are two different fission valleys leading to two distinctly different scission configurations, one conventional scission configuration of two fairly elongated shapes corresponding to the low kinetic-energy peak and one compact scission configuration of two touching spheres corresponding to the high kinetic-energy peak.

The valley leading to the compact scission configuration of two touching spheres becomes prominent close to $^{258}$Fm because of the large negative shell corrections in fragments close to $^{132}$Sn. The shell correction of $^{132}$Sn is about $-13$ MeV. Thus the configuration of two touching $^{132}$Sn nuclei has a shell correction of $-26$ MeV. Configurations close to doubly magic configurations are also expected to have substantial shell corrections. The configuration of two touching $^{129}$Sn nuclei, corresponding to symmetric fission of $^{258}$Fm, has a shell correction of $-18$ MeV.

As the first step in our study of the possibility of multiple valleys in the potential-energy surface we select a set of shapes for which to calculate the potential energy. Our choice is shown in fig. 3. This choice includes ground-state shapes in the lower left corner, shapes leading to elongated scission configurations in the upper right corner, and shapes corresponding to compact scission configurations in the lower right part of the figure. In the caption to this figure and throughout this paper we use units in which the spherical radius $R_0 = 1$.

The result of the calculation is seen in fig. 4. Some structures seen in this potential-energy surface are: a ground state at $r = 0.86$ with potential energy $E = -4$ MeV, a first saddle at $r = 1.0$ with $E = 4$ MeV, and a second minimum at $r = 1.3$ and $\sigma = 0.70$ with $E$ slightly below $-2.0$ MeV. The dot-dashed line leads along the conventional old path into a valley that ends at an elongated scission configuration. The short-dashed line leads over a saddle that corresponds to shapes close to two touching spheres and into a new fission valley.

Spontaneous-fission half-lives are extremely sensitive to small changes in the barrier energies. The fact that both low and high kinetic-energy fission are observed simultaneously for several fissioning species shows that the penetrability through the two barriers leading to these two configurations must be very similar. That two completely different barriers have similar penetrabilities is extremely unlikely. Therefore, in our interpretation, the branching into the different valleys must take place at a late stage during the penetration process. Figure 4 shows that a third long-dashed path branches off from the new path at about $r = 1.45$ and $\sigma = 0.70$. This path, which

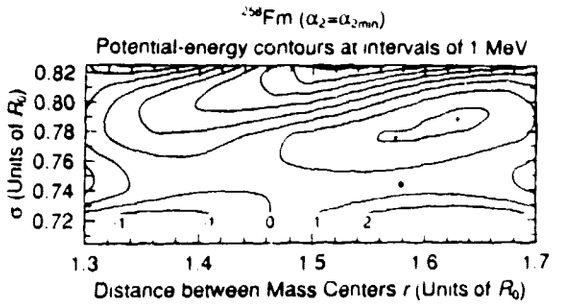


Figure 6: Potential energy minimized with respect to the mass-asymmetry coordinate $\alpha_2$. The height of the switchback saddle at $r = 1.4$ and $\sigma = 0.75$ is now about the same as the outer saddle on the new path at $r = 1.6$ and $\sigma = 0.74$.

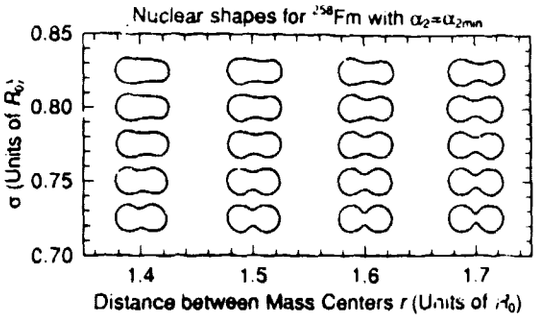


Figure 7: Nuclear shapes corresponding to the potential-energy surface in fig. 6.

we call the *switchback path*, leads back into the old valley across a third saddle at $r = 1.5$ and $\sigma = 0.825$. The barrier between the ground state and the new and old valleys along the new and switchback paths differ only along a small portion near the end part of the barrier. Thus the barriers and the corresponding penetrabilities are not much different, which explains the mechanism behind the simultaneous observations of low and high kinetic-energy fission.

The new fission valley is most prominent close to $^{264}$Fm. In fig. 5 we show a potential-energy surface for $^{252}$Cf. Here access to the new valley is blocked by a high ridge. The outer saddle on the old path is now the lowest saddle. However, microscopic effects on the inertia have to be considered to determine whether the nucleus follows the old or the switchback path into the old valley.

The effect of mass-asymmetric distortions is not included in fig. 4. We have studied [21] this shape degree of freedom at all three outer saddle points of the potential-energy surface, but show here only the results for the shaded region in fig. 4, for which we have performed a full three-dimensional calculation. For each $r$ and $\sigma$ we have minimized the energy with respect to the mass-asymmetry coordinate. The minimized energy is shown as a function of $r$ and $\sigma$ in fig. 6 and the corresponding shapes in fig. 7. The inclusion of mass-asymmetry leaves the saddle on the new path unaffected but lowers the saddle on the switchback path by more than 2 MeV so that the two saddle-point heights are now approximately equal. The shapes remain clearly symmetric along the new path, but mass asymmetry sets in and grows along the switchback path towards the old valley.

Spontaneous-fission half lives are related to an integral along the fission path involving the product of the fission-barrier height and the inertia associated with the motion through the barrier. Since the half-life is an invariant, independent of the choice of shape coordinates, the inertia clearly depends on the choice of coordinate system. It also depends on the internal structure of the system. A large amount of internal reorganization, which occurs at level crossings, raises the inertia. In the coordinate system we choose, distance between mass centers, the inertia for separated fragments should be equal to the reduced mass. For shapes near the ground state the inertia is expected to be considerably above the value corresponding to irrotational flow. A consideration of these limits led ref. [15] to propose a semi-empirical model for the inertia. In this model the inertia is

$$B_r = k(B_r^{\rm irr} - \mu) + \mu \qquad (2)$$

where $k$ is an adjustable constant, $B_r^{\rm irr}$ is the irrotational inertia and $\mu$ the reduced mass of the separated fragments. Figure 8 taken from ref. [25] shows the inertia in this model and two curves obtained in a microscopic cranking-model calculation. The short-dashed (static) curve corresponds to a fission path that is selected as straight lines between the minima and saddle points. The solid (dynamic) curve corresponds to a path that maximizes the penetrability.

There are strong microscopic effects in the cranking-model calculations. Spontaneous-fission half-life calculations based on the cranking model and on the semi-empirical model for the inertia agree about equally well with experimental data. An explanation for the good results obtained in the semi-empirical approach is probably that the integration of the product of the cranking-model inertia and the barrier height along the fission path washes out the microscopic fluctuations. The search for a path with maximum penetrability also decreases the amplitude of the fluctuations in the cranking model inertia, as is seen in fig. 8.

The fluctuations in the level structure do not, on the average, depend critically on the particular nucleus considered for fission along the old path. Therefore, the same semi-empirical inertia is used for all actinide nuclei for half life calculations along the old path. However, along the new path the single-particle level spectrum is very

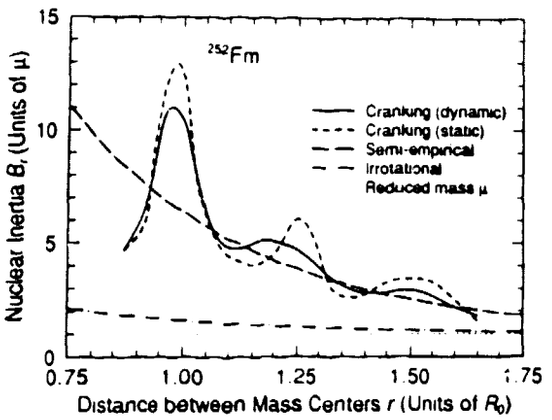


Figure 8: Nuclear inertia in microscopic, semi-empirical, and hydrodynamical models.

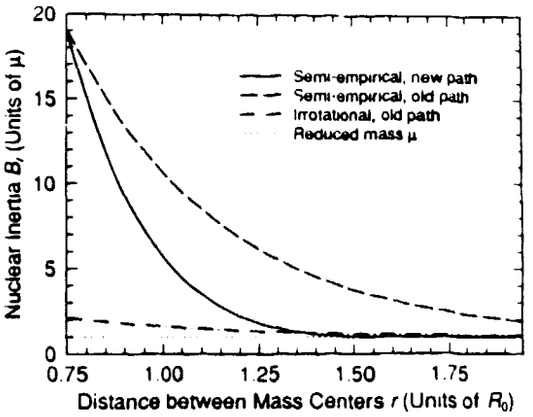


Figure 9: Semi-empirical inertia along the old and new fission paths.

different[21] from the level spectrum along the old path. Already slightly beyond the *first* saddle fig. 3 shows that the fragments become developed, which in the level diagram corresponds to levels that change very little with deformation beyond the first saddle. Therefore, the inertia along the new path is expected to approach the reduced mass much more rapidly than along the old path. This is discussed in greater detail in ref. [22] from which we take fig. 9, where the semi-empirical inertias corresponding to the old and new paths are displayed.

Calculated spontaneous-fission half-lives are displayed in fig. 10. The calculations are based on the semi-empirical inertia displayed in fig. 9 and calculated potential-energy surfaces similar to the one shown in fig. 4. Mass-asymmetric shape degrees of freedom were taken into account at the outer saddle points. When a new path is present in the calculated surfaces spontaneous-fission half-lives have been calculated along both the old and new paths. The shorter half-life corresponds to the designation dominating path in fig. 10. When the new path is present it is always the dominating path for the cases displayed in fig. 10.

There are some large disagreements between the calculated and experimental half-lives, in particular close to $N = 152$. Since a change in the ground-state energy by 1 MeV changes the calculated half-life by six orders of magnitude, an error of 1 MeV in the calculated ground-state energy at $N = 152$ would explain the discrepancy. Another possible explanation is that fission proceeds along the switchback path, but this has not been investigated theoretically at this time.

The configuration of two touching spheres is reached already at $r = 1.59$. For $^{258}$Fm the barrier along the new path is not yet penetrated at this small $r$ value because at this configuration we are dealing with two separate nuclei it is important that the shape dependences of the model used are such that the same energy is obtained whether the configuration is treated as *one* highly deformed $^{258}$Fm system or as *two* touching $^{129}$Sn nuclei. Because earlier calculations seldom followed a system through such radical shape changes that the system evolved from a single system to two separated nuclei, the usual formulations of the models have deficiencies in this respect. Our results here have been obtained with models that have been extended[22] to include shape dependences for the particularly important Wigner and $A^0$ terms.

The calculations of a Polish group[26] treat these terms as independent of deformation. This leads to a deeper new valley for $^{258}$Fm in their calculation. In fact their results show that there is no second barrier for this nucleus. In their view the mechanism behind the short half-life of $^{258}$Fm is the *disappearance* of the second barrier.

In our view, the condition that the same energy be obtained regardless of whether the system is treated as a single, highly deformed one or as two touching spherical nuclei *has* to be fulfilled. With this condition met we find that the mechanism behind the steep decrease of half-lives of Fm isotopes beyond $N = 152$ is the rapid deepening of the new valley floor with increasing $N$, coupled with a lower inertia in the new valley than in the old valley.

The differences between the models have important consequences for the predicted properties of very neutron-rich elements. The calculations of the Polish group[27,28] show increased stability as $N = 162$ is approached, whereas we find that the stability in this region is also affected by the appearance of the new valley.

In our approach the new valley in the potential-energy surface destabilizes the heaviest elements. Figure 10 shows that the calculated half-life along the new path is about 10 orders of magnitude shorter than along the old path for $N \geq 160$. The neutron number $N = 162$ is

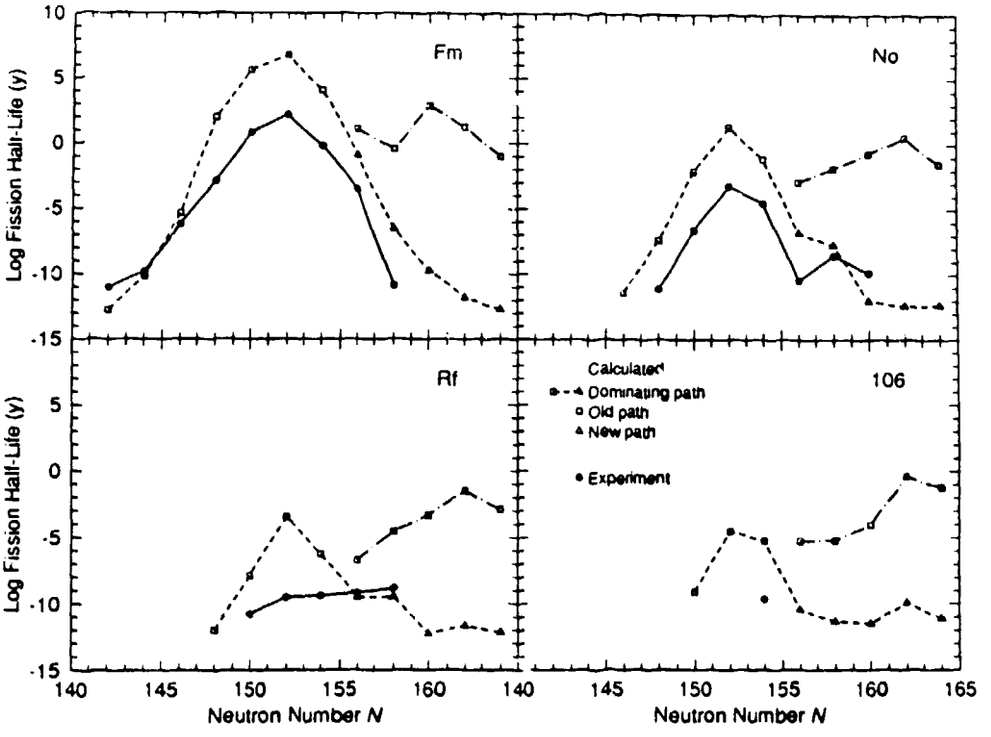


Figure 10: Calculated spontaneous-fission half-lives compared to experimental data.

associated with a gap in the calculated level spectrum for deformed shapes. It has been assumed that elements in the vicinity of this neutron number are unusually stable. The recent discoveries[29,30] of elements with proton number up to $Z = 109$ show that these elements have a ground-state shell correction of about $-6$ MeV. The theoretical predictions of a deformed neutron shell at $N = 162$ have led to the expectation that the stability would increase as this neutron number is approached. However, we now see that the stability is not solely determined by the *ground-state* shell gap at $N = 162$. The more complete picture is that the fission properties are affected by the balance between the stabilizing influence of the $N = 162$ *ground-state* shell gap and the destabilizing influence of the *fragment* $N = 2 \times 82 = 164$ shell gap.

## PAST AND FUTURE

The past has seen the models for the fission barrier evolve from a simple liquid-drop model, which was the dominating model for the first 25 years, to a more complex picture in which the calculation of shell effects adds a rich structure to the potential-energy surface. Instead of interpreting fission in terms of a one-dimensional barrier, we now interpret the fission process for $^{258}$Fm, for example, in terms of a multi-dimensional potential-energy surface on which we have identified a large number of important features: a ground-state minimum separated from a second minimum by a first barrier peak, a second minimum beyond which two saddles lead to a conventional and a new fission valley, and a switchback path that leads from the new valley across a third outer saddle back to the old, conventional fission valley.

Twenty-five years ago Wilets[31] said about the liquid-drop model, "Despite its basic simplicity, it remains basically unexplored." Since then, finite-range effects have been incorporated to generalize the description of the surface-energy. But other features, notably the Wigner term and its shape dependence which have effects on the potential-energy surface of up to 10 MeV, remain poorly understood. Studies of the new fission valley show that it is crucial to achieve an improved understanding of the origins of this term and its shape dependence in order to reliably calculate the potential-energy surface in the scission region.

The evolution of the shape of the nucleus along the three paths on the potential-energy surface corresponds to radically different rearrangements of internal structure. This in turn leads to large differences in the inertia along the several fission paths. More extensive theoretical studies of microscopic effects on the inertia would improve our understanding of the fission properties in the Fm region.

The theoretical efforts to understand the forces that

balance the nucleus against disruption at the very end of the peninsula of known nuclei would be greatly aided by experiments that study nuclei with $N \geq 160$. The future certainly holds a promise of a deeper understanding of the properties of nuclei close to $^{264}$Fm. As our understanding of this pool of instability evolves, it will increase our ability to reach for what is beyond, be it rocks or a super-heavy island. Undoubtedly, the future will see exciting new discoveries in the waters beyond the end of the peninsula of known elements.

ACKNOWLEDGEMENT

This work was supported by the U. S. Department of Energy.

REFERENCES

1. I. Noddack, Angew. Chem. **47** (1934) 653.
2. L. Meitner and O. R. Frisch, Nature **143** (1939) 239, 471.
3. N. Bohr and J. A. Wheeler, Phys. Rev. **56** (1939) 426.
4. W. J. Swiatecki, Phys. Rev. **100** (1955) 937.
5. J. O. Newton, Prog. Nucl. Phys. **4** (1955) 234.
6. J. A. Wheeler, Nuclear fission and nuclear stability, in Niels Bohr and the development of physics: Essays dedicated to Niels Bohr on the occasion of his seventieth birthday (Pergamon, London, 1955) p. 163.
7. S. A. E. Johansson, Nucl. Phys. **12** (1959) 449.
8. V. M. Strutinsky, Nucl. Phys. **A95** (1967) 420.
9. V. M. Strutinsky, Nucl. Phys. **A122** (1968) 1.
10. P. Möller and S. G. Nilsson, Phys. Lett. **31B** (1970) 283.
11. H. C. Pauli and T. Ledergerber, Proc. Third IAEA Symp. on the physics and chemistry of fission, Rochester, 1973, vol. I (IAEA, Vienna, 1974) p. 463.
12. J. Randrup, C. F. Tsang, P. Möller, S. G. Nilsson, and S. E. Larsson, Nucl. Phys. **A217** (1973) 221.
13. S. G. Nilsson, C. F. Tsang, A. Sobiczewski, Z. Szymański, S. Wycech, C. Gustafson, I.-L. Lamm, P. Möller, and B. Nilsson, Nucl. Phys. **A131** (1969) 1.
14. M. Brack, J. Damgaard, A. S. Jensen, H. C. Pauli, V. M. Strutinsky, and C. Y. Wong, Rev. Mod. Phys. **44** (1972) 185.
15. E. O. Fiset and J. R. Nix, Nucl. Phys. **A193** (1972) 647.
16. W. D. Myers and W. J. Swiatecki, Ark. Fys. **36** (1967) 343.
17. W. D. Myers and W. J. Swiatecki, Ann. Phys. (N. Y.) **55** (1969) 395.
18. W. D. Myers and W. J. Swiatecki, Ann. Phys. (N. Y.) **84** (1974) 186.
19. H. J. Krappe, J. R. Nix, and A. J. Sierk, Phys. Rev. **C20** (1979) 992.
20. J. Błocki, J. Randrup, W. J. Swiatecki, and C. F. Tsang, Ann. Phys. (N. Y.) **105** (1977) 427.
21. P. Möller, J. R. Nix, and W. J. Swiatecki, Nucl. Phys. **A469** (1987) 1.
22. P. Möller, J. R. Nix, and W. J. Swiatecki, Nucl. Phys. **A** (1989), to be published.
23. Proc. Third IAEA Symp. on the physics and chemistry of fission, Rochester, 1973, vols. I, II (IAEA, Vienna, 1974).
24. E. K. Hulet, J. F. Wild, R. J. Dougan, R. W. Lougheed, J. H. Landrum, A. D. Dougan, M. Schädel, R. L. Hahn, P. A. Baisden, C. M. Henderson, R. J. Dupzyk, K. Sümmerer, and G. R. Bethune, Phys. Rev. Lett. **56** (1986) 313.
25. A. Baran, K. Pomorski, S. E. Larsson, P. Möller, S. G. Nilsson, J. Randrup, A. Lukasiak, and A. Sobiczewski, Proc. 4th IAEA Symp. on physics and chemistry of fission, Jülich, 1979, vol. I (IAEA, Vienna, 1980) p. 143.
26. S. Ćwiok, P. Rozmej, A. Sobiczewski, and Z. Patyk, Nucl. Phys. **A469** (1989) 281.
27. K. Böning, Z. Patyk, A. Sobiczewski, and S. Ćwiok, Z. Phys. **A325** (1986) 479.
28. A. Sobiczewski, Z. Patyk, and S. Ćwiok, Phys. Lett. **B183** (1987) 6.
29. P. Armbruster, Ann. Rev. Nucl. Part. Sci. **35** (1985) 135.
30. G. Münzenberg, Rep. Prog. Phys. **51** (1988) 57.
31. L. Wilets, Theories of nuclear fission (Clarendon Press, Oxford, 1964).